ELECTRONICS AND ELECTRICAL ENGINEERING
ISSN 1392 – 1215 2009. No. 6(94)
ELEKTRONIKA IR ELEKTROTECHNIKA

T191 HIGH FREQUENCY TECHNOLOGY, MICROWAVES
AUKŠTŲJŲ DAŽNIŲ TECHNOLOGIJA, MIKROBANGOS

Dependences of Propagation Constants of Cylindrical n-Si Rod on the Material Specific Resistivity

S. Asmontas, L. Nickelson, D. Plonis
Semiconductor Physics Institute, Teraherzt's Electronics Laboratory,
A. Gostauto g. 11, LT–01108 Vilnius, Lithuania, phone: +370 5 2627124; e-mail: asmontas@pfi.lt

Introduction

Circular rod waveguides for many years were investigated due to their excellent electrodynamical characteristics like a large broadbandwidth and the wide possibilities for their implementation in microwave devices and solid-state electronics.

Circular semiconductor and ferrite rod waveguides placed into the longitudinal magnetic fields were studied in [1]. The dispersion characteristic analyze of circular *p*-Ge, *p*-Si and *n*-InSb plasma rod waveguides at several free charge carrier concentrations was made in [2, 3]. The investigation of dielectric and metamaterial rod and hollow-core waveguides were presented in [4]. Rod waveguides are successfully used in microwave devices such as filters, isolators and others [5–8].

Here we present the dispersion characteristic analysis of circular semiconductor *n*-Si rod waveguides (Fig. 1) dependent on the waveguide radius and the material specific resistivity.

We have investigated the complex longitudinal propagation constants, the transversal propagation constants of the waveguide in the wide frequency range from 15 to 300GHz.

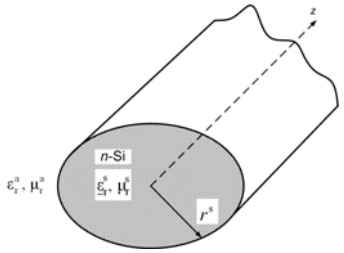

Fig. 1. The cylindrical semiconductor n-Si waveguide model

Calculation algorithm

For the solution of our electrodynamical problem we used Maxwell's equations in this form:

$$\nabla\times\underline{\boldsymbol{E}}=-\mathrm{i}\omega\mu_r^s\mu_0\underline{\boldsymbol{H}};\qquad \nabla\times\underline{\boldsymbol{H}}=\mathrm{i}\omega\underline{\varepsilon}_r^s\varepsilon_0\underline{\boldsymbol{E}},\qquad (1)$$

where $\underline{\boldsymbol{H}}$ – the magnetic field strength; $\underline{\boldsymbol{E}}$ – the electric field strength. The magnitude $\underline{\varepsilon}_r^s=\varepsilon_r^{s\prime}-\mathrm{i}\varepsilon_r^{s\prime\prime}$ is the complex permittivity of the *n*-Si semiconductor, where the real part is $\varepsilon_r^{s\prime}=\mathrm{Re}(\underline{\varepsilon}_r^s)$ and the imaginary part is $\varepsilon_r^{s\prime\prime}=\mathrm{Im}(\underline{\varepsilon}_r^s)$. It is known that the last magnitude dependent on the frequency:

$$\varepsilon_r^{s\prime\prime}=\frac{1}{\omega\varepsilon_0\rho},\qquad (2)$$

where the value ρ is the semiconductor material specific resistivity. The magnitude $\mu_r^s=1$ is the semiconductor permeability. The magnitudes $\varepsilon_r^a=1$ and $\mu_r^a=1$ are the permittivity and permeability of air.

The dispersion equation of the semiconductor waveguide is:

$$\begin{aligned}\underline{\Delta}=&\,\omega^2\varepsilon_0\mu_0\underline{\eta}\left(\underline{\chi}'\right)^2\underline{\Delta}_s^2\left(r^s\right)^2\left(\underline{k}_\perp^a\right)^2-m^2\underline{h}^2\underline{\eta}\underline{\chi}^2\underline{\Delta}_s^2-\\&-\mathrm{i}m^2\underline{h}\underline{\eta}\underline{\chi}^2\underline{f}_2\underline{\Delta}_s\left(\underline{k}_\perp^a\right)+\mathrm{i}\omega\mu_0\underline{\chi}\underline{\chi}'\underline{\eta}'\underline{s}_1\underline{\Delta}_s\left(r^s\right)^2\underline{k}_\perp^s\left(\underline{k}_\perp^a\right)^3+\\&+\mathrm{i}\omega\varepsilon_0\underline{\chi}'\underline{\eta}\underline{\eta}'\underline{f}_1\underline{\Delta}_s\left(r^s\right)^2\underline{k}_\perp^s\left(\underline{k}_\perp^a\right)^3+\\&+\underline{\chi}\left(\underline{\eta}'\right)^2\underline{f}_1\underline{s}_1\left(r^s\right)^2\left(\underline{k}_\perp^s\right)^2\left(\underline{k}_\perp^a\right)^4+\mathrm{i}m^2\underline{h}\underline{\eta}^2\underline{\chi}\underline{f}_2\underline{\Delta}_s\left(\underline{k}_\perp^a\right)^2-\\&-m^2\underline{\eta}^2\underline{\chi}\underline{f}_2^2\left(\underline{k}_\perp^a\right)^4=0,\end{aligned}\qquad (3)$$

where $\underline{\eta}=\mathrm{J}_m(\underline{k}_\perp^s r)$ – the Bessel function of the *m*-th order; $\underline{\chi}=\mathrm{H}_m^{(2)}(\underline{k}_\perp^a r^s)$ – the Hankel function of the second kind; $\underline{\eta}'$, $\underline{\chi}'$ – derivatives of magnitudes $\underline{\eta}$ and $\underline{\chi}$; $\underline{k}_\perp^s=\sqrt{k^2\underline{\varepsilon}_r^s\mu_r^s-\underline{h}^2}$ – the transversal propagation constant for the semiconductor medium; r^s – the waveguide radius; $\underline{k}_\perp^a=\sqrt{\underline{h}^2-k^2\underline{\varepsilon}_r^a\mu_r^a}$ – the transversal propagation constant in air; m is the azimuthal index. The value

$\underline{\Delta}_s = \left(\underline{k}_\perp^s\right)^4$, $k = \omega/c$ – the wave number in a vacuum, $\omega = 2\pi f$, where f – an operating frequency, $\underline{s}_1 = \mathrm{i}\,\omega\,\varepsilon_0\,\underline{\varepsilon}_r^s\left(\underline{k}_\perp^s\right)^2$, $\underline{f}_1 = \mathrm{i}\omega\mu_0\underline{\mu}_r^s\left(\underline{k}_\perp^s\right)^4$, $\underline{f}_2 = \mathrm{i}\underline{h}\left(\underline{k}_\perp^s\right)^2$.

The complex longitudinal propagation constant $\underline{h}$ can be written $\underline{h} = h' - \mathrm{i}h''$, where $h' = \mathrm{Re}(\underline{h})$ is the real part of the complex longitudinal propagation constant, $h'' = \mathrm{Im}(\underline{h})$ is the imaginary part of the complex longitudinal propagation constant. The expression of real part of the complex longitudinal propagation constant $h' = \dfrac{2\pi}{\lambda_w}$, where λ_w – the wavelength of the waveguide modes. In our calculations an azimuthal index is $m = 1$.

We use the Muller method for searching of complex roots of the dispersion equation (3).

Dispersion characteristic analysis

We have investigated the *n*-Si waveguide dispersion characteristics for four sets of parameters of the waveguide. Our calculations have been executed for two material specific resistivity ρ and two waveguide radii r^s. Values ρ were equal to $0.3\ \Omega\cdot\mathrm{m}$ and $300\ \Omega\cdot\mathrm{m}$. We see that the value of material specific resistivity differ in 1000 times. Radii of investigated waveguides were 0.25 mm and 1mm. We accepted in our calculations that the value $\varepsilon_r^{s\prime\prime} = 3.9$ at the frequency $f = 15.4$ GHz. Our calculations of the values h' and h'' are presented in Figs 2 – 5. The real and imaginary parts of value $\underline{k}_\perp^a$ are shown in Figs. 6 and 7. The values of h' and $\mathrm{Re}(\underline{k}_\perp^a)$ are normalized to the value k in Figs 2, 4, 6.

Here we presented the results of our examination of two hybrid modes HE_{11} and EH_{11}. The mode HE_{11} is the main mode and the mode EH_{11} is the first higher mode of the open *n*-Si semiconductor rod waveguide. The curves noted by points correspond to the waveguide with the radius $r^s = 0.25$ mm. The curves designated by circles correspond to the waveguide with the radius $r^s = 1$ mm.

In Fig. 2 we presented h' when $\rho = 0.3\ \Omega\cdot\mathrm{m}$, radii $r^s = 0.25$ mm (circles) and 1mm (points).

We see that dispersion characteristics of waveguides with different radii are considerably various. The behavior of dispersion characteristics of *n*-Si rods with various radii especially differ in the area of the cutoff frequency. The dispersion characteristic of mode HE_{11} at the waveguide radius 0.25 mm is almost parallel f-axis in the frequency range from 15 to 100 GHz. It means that the wavelength of the *n*-Si rod with the radius 0.25 mm does not depend on the frequency in the wide frequency range.

We see that losses sharply increase in the area of the cutoff frequency of HE_{11} mode when waveguide radius is 1 mm. The inclination of the curve h' rapidly increased in the area of f_{cut} (see Fig. 2) too. The both cutoff frequencies of the EH_{11} modes are located in the area where the parameter $h'/k < 1$. Though the working part of dispersion curves located in the area where the parameter $h'/k > 1$.

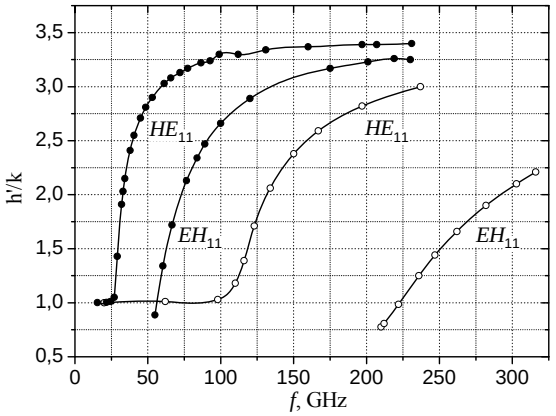

Fig. 2. Dependences of real part of the complex longitudinal propagation constant on the frequency for two modes, when $\rho = 0.3\ \Omega\cdot\mathrm{m}$

The broadbandwidths of waveguides with $r^s = 0.25$ mm and 1 mm approximately equal to 61% and 62% respectively.

In Fig. 3 is shown losses of modes HE_{11} and EH_{11} at two radii 0.25 mm (points) and 1 mm (circles).

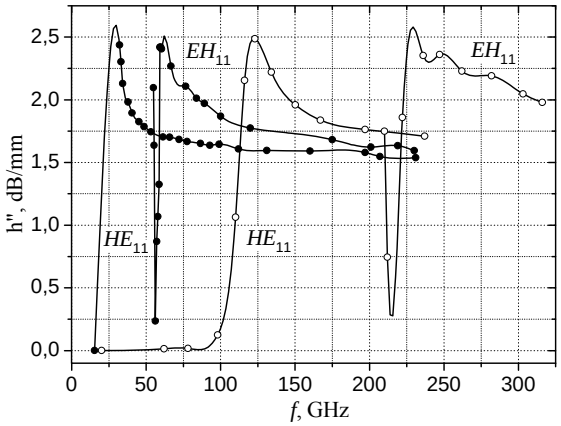

Fig. 3. Dependences of imaginary part of the complex longitudinal propagation constant on the frequency for two modes when $\rho = 0.3\ \Omega\cdot\mathrm{m}$

The losses of the mode HE_{11} when the waveguide radius is 0.25 mm are small in the frequency range from 15 to 100 GHz. It is possible to explain by the fact that the magnitude $h'/k \approx 1$ in this frequency range. It leads that the largest part of the electromagnetic energy extends outside of *n*-Si rod. The losses' minimum closed to f_{cut} of EH_{11} modes when radii 0.25 mm and 1 mm is possible to explain by a conception that these modes have $h'/k < 1$. The most portion of the EH_{11} mode' electromagnetic energy concentrates outside of the *n*-Si rod where losses are small.

In Fig. 4 is presented h' when $\rho = 300\ \Omega\cdot\mathrm{m}$, radii $r^s = 0.25$ mm (circles) and 1 mm (points).

The comparison of the dispersion characteristics in Fig. 2 and Fig. 4 shows that the influence of material specific

resistivity on the real part of the complex longitudinal propagation is weak.

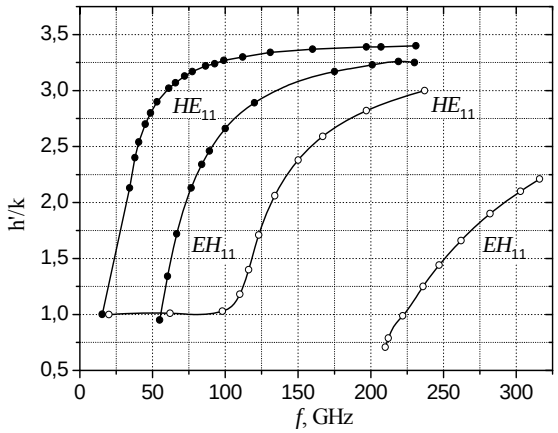

Fig. 4. Dependences of real part of the complex longitudinal propagation constant on the frequency for two modes, when $\rho = 300\ \Omega \cdot \mathrm{m}$

The losses of modes HE_{11} and EH_{11} at two radii 0.25 mm (points) and 1 mm (circles) is demonstrated in Fig. 5.

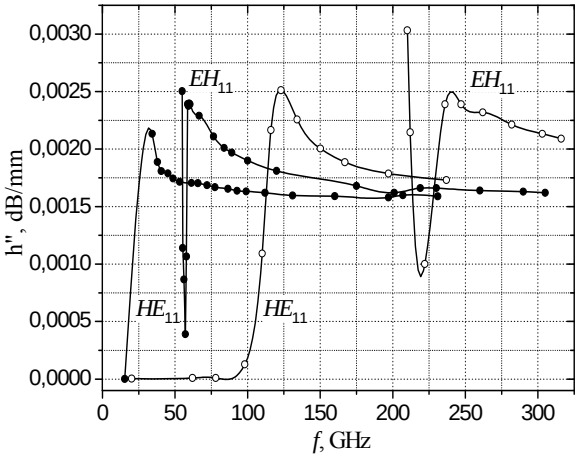

Fig. 5. Dependences of imaginary part of the complex longitudinal propagation constant on the frequency for two modes when $\rho = 300\ \Omega \cdot \mathrm{m}$

We see that when the material specific resistivity is large ($\rho = 300\ \Omega \cdot \mathrm{m}$) the losses become extremely small. The comparison of Figs 3 and 5 shows when the specific resistivity changes from $0.3\ \Omega \cdot \mathrm{m}$ till $300\ \Omega \cdot \mathrm{m}$ the losses can decrease more than in 1000 times.

In Fig. 6 and Fig. 7 are presented the real and imaginary parts of the complex transversal propagation constant in air of the HE_{11} and EH_{11} modes at two radii 0.25 mm (points) and 1 mm (circles) when $\rho = 0.3\ \Omega \cdot \mathrm{m}$.

The value $\mathrm{Re}(\underline{k}_{\perp}^{\mathrm{a}})$ describes speed of the electromagnetic energy attenuation of a mode outside of the waveguide. The larger is $\mathrm{Re}(\underline{k}_{\perp}^{\mathrm{a}})$ the larger part of electromagnetic mode energy propagates inside of the *n*-Si rod. We can see that the position of $\mathrm{Re}(\underline{k}_{\perp}^{\mathrm{a}})$ curves' maximums coincide with the position of the loss curves' maximums on a scale of frequencies Fig. 3 and Fig. 5.

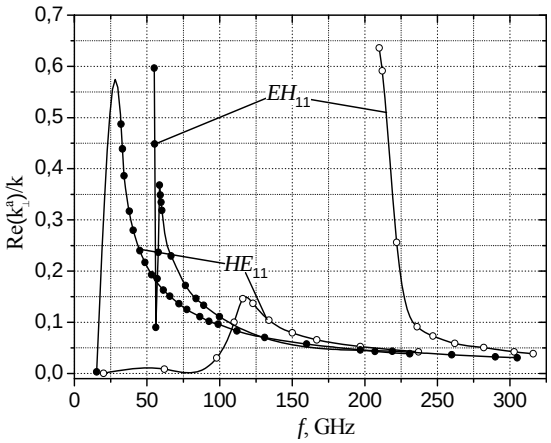

Fig. 6. Dependences of real part of the complex transversal propagation constant in air on the frequency for two modes, when $\rho = 0.3\ \Omega \cdot \mathrm{m}$

The behavior of the similar characteristics $\mathrm{Re}(\underline{k}_{\perp}^{\mathrm{a}})$ when $\rho = 300\ \Omega \cdot \mathrm{m}$ is analogical to Fig.6. Magnitudes of $\mathrm{Re}(\underline{k}_{\perp}^{\mathrm{a}})$ when $\rho = 300\ \Omega \cdot \mathrm{m}$ compare to $\mathrm{Re}(\underline{k}_{\perp}^{\mathrm{a}})$ when $\rho = 0.3\ \Omega \cdot \mathrm{m}$ are differ in 1000 times but the curves' behavior is the same.

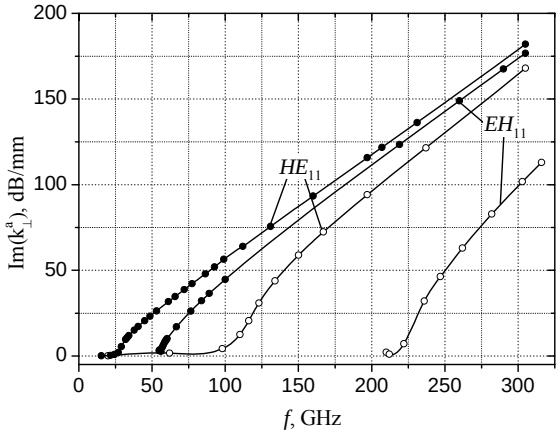

Fig. 7. Dependences of imaginary part of the complex transversal propagation constant in air on the frequency for two modes, when $\rho = 0.3\ \Omega \cdot \mathrm{m}$

The magnitude $\mathrm{Im}(\underline{k}_{\perp}^{\mathrm{a}})$ influences most considerably on the behavior and value of *h*' (Fig. 2). Here we do not placed the $\underline{k}_{\perp}^{\mathrm{a}}$ characteristics when $\rho = 300\ \Omega \cdot \mathrm{m}$. Because the values and behaviors of $\mathrm{Im}(\underline{k}_{\perp}^{\mathrm{a}})$ as well as the behaviors of $\mathrm{Im}(\underline{k}_{\perp}^{\mathrm{a}})$ are the same for *n*-Si rods with $\rho = 0.3\ \Omega \cdot \mathrm{m}$ and $\rho = 300\ \Omega \cdot \mathrm{m}$.

Conclusions:

1. We investigated the dependences of *n*-Si rod waveguides' dispersion characteristics at two material specific resistivity ($0.3\ \Omega \cdot \mathrm{m},\ 300\ \Omega \cdot \mathrm{m}$) and two radii ($0.25\,\mathrm{mm}, 1\,\mathrm{mm}$) in the wide range 15-300 GHz of frequencies.

2. The behavior of dispersion characteristics of *n*-Si rods with various radiuses especially differ in the area of the cutoff frequency.

3. The dispersion characteristic of mode HE_{11} at the waveguide radius 0.25 mm is independent on the frequency in the range from 15 to 100 GHz.

4. The waveguide losses sharply decreas when the real part of the complex longitudinal propagation constant is less than the wave number in a vacuum.

References

1. **Nickelson L., Asmontas S., Malisauskas V., Shugurov V.** The open cylindrical gyrotropic waveguides. – Vilnius: Technika, 2007. – 248 p. (in Lithuanian).
2. **Asmontas, S., Nickelson, L., Malisauskas, V.** Investigation of Magnetized Semiconductor and Ferrite Waveguides // Elektronika ir elektrotechnika. Kaunas: Technologija, 2006. – No. 2(66). – P. 56–61. (in Lithuanian)
3. **Nickelson L., Asmontas S., Malisauskas V., Martavicius R.** The dependence of open cylindrical magnetoactive *p*–Ge and *p*–Si plasma waveguide mode cutoff frequencies on hole on concentrations. //J. Plasma Physics, 2009. – No 1 (75). – P. 35–51.
4. **Nickelson L., Gric T., Asmontas S., Martavicius R.** Electrodynamical analyses of dielectric and metamaterial hollow–core cylindrical waveguides // Electronics and Electrical Engineering, 2008. – No. 2(82). – P. 3–8.
5. **Safavi–Naeini S., Chaudhuri S. K., Goss A.** Design and Analysis of Novel Multimode Optical Filters in Dielectric Waveguide // J. of lightwave technology, 1993. – No. 12(11). – P. 1970–1977.
6. **Kanda M. , May W. G.** New millimetre–wave isolator containing a semiconductor rod in a circular waveguide // Electronics Letters, 1975. – No. 12(11). – P. 261–262.
7. **Jankauskas Z., Kvedaras V.** Electrical Field and Current Distribution in Semiconductor Plasma in the Strong Magnetic Field // Elektronika ir elektrotechnika. Kaunas: Technologija, 2007. – No. 2(74). – P. 41–44.
8. **Skudutis J., Daskevic V.** Investigation of Meander Delay System Properties using the „MicroWave Studio“ Software Package // Elektronika ir elektrotechnika. Kaunas: Technologija, 2006. – No. 8(72). – P. 11–15.

Received 2009 02 15

S. Asmontas, L. Nickelson, D. Plonis. Dependences of Propagation Constants of Cylindrical n-Si Rod on the Material Specific Resistivity // Electronics and Electrical Engineering. – Kaunas: Technologija, 2009. – No. 6(94). – P. 57–60.

In the present work the dispersive dependences of cylindrical *n*-Si rod waveguides are analyzed at two specific resistivity of a semiconductor material ($0.3\,\Omega\cdot\mathrm{m}$, $300\,\Omega\cdot\mathrm{m}$) and at two waveguide radii (0.25 mm, 1 mm) for the basic HE_{11} and the first higher EH_{11} hybrid modes. Muller's method has been used for complex roots' searching of the dispersive equation. Here is presented the broadbandwidths of waveguides of investigated *n*-Si rod waveguides. It is established that for investigated waveguides the broadbandwidths of waveguides almost coincide. Here are presented dependences of complex longitudinal propagation constants and the transversal propagation constants in air on a wide interval of frequencies from 15 to 300 GHz. It is established that character of dispersive curves in area of the cutoff frequency is strongly depends on the waveguide radius. The wavelength of mode HE_{11} of *n*-Si rod waveguide with the radius equal to 0.25 mm in the frequency range from 15 GHz to 100 GHz is independent on the frequency. It is shown that in frequency intervals where a real part of complex longitudinal propagation constants becomes less than a wave number in air, it is observed sharp decreasing of waveguide losses. Ill. 7, bibl. 8 (in English; abstracts in English, Russian and Lithuanian).

С. Ашмонтас, Л. Никельсон, Д. Плонис. Зависимость постоянной распространения цилиндрических n-Si стержневых волноводов от удельного сопротивления материала // Электроника и электротехника. – Каунас: Технология, 2009. – № 6(94). – С. 57–60.

В настоящей работе проанализированы дисперсионные зависимости цилиндрических *n*-Si стержневых волноводов при двух значениях удельного сопротивления полупроводникового материала ($0{,}3\,\Omega\cdot$м, $300\,\Omega\cdot$м) и при двух значениях радиусов волновода (0,25 мм, 1 мм) для основной HE_{11} и первой высшей EH_{11} гибридных волн. Для обнаружения комплексных корней дисперсионного уравнения был использован метод Мюллера. Показана широкополосность исследуемых *n*-Si стержневых волноводов. Установлено, что для исследуемых волноводов широкополосности почти совпадают. Значения реальных и мнимых составляющих комплексной продольной постоянной распрострнения, а также поперечной постоянной распространения в воздухе приведены для широкого интервала частот – от 15 до 300 ГГц. Установлено, что характер дисперсионных кривых в области отсечки сильно зависит от радиуса волновода. Для моды HE_{11} волновода с радиусом равным 0,25 мм обнаружена область частот от 15 ГГц до 100 ГГц, в которой длина волны в волноводе остается неизменной при изменении частоты. Показано, что в частотных интервалах, где реальная часть комплексной продольной постоянной распространения h' становится меньше волнового числа k, наблюдается резкое уменьшение потерь в волноводе. Ил. 7, библ. 8 (на английском языке; рефераты на английском, русском и литовском яз.).

S. Ašmontas, L. Nickelson, D. Plonis. Cilindrinio n-Si strypo sklidimo konstantos priklausomybė nuo medžiagos savitosios varžos // Elektronika ir elektrotechnika. – Kaunas: Technologija, 2009. – Nr. 6(94). – P. 57–60.

Ištirtos cilindrinių *n*-Si bangolaidžių dispersines charakteristikas dviejų skirtingų spindulių (0,25 mm, 1 mm) esant dviems skirtingoms puslaidininkio savitosioms varžoms $(0{,}3\,\Omega\cdot\mathrm{m}, 300\,\Omega\cdot\mathrm{m})$ bei pagrindinė HE_{11} ir pirmoji aukštesnioji EH_{11} hibridinės bangos. Dispersinės lygties kompleksinių šaknų paieškai buvo taikomas *Muller*io metodas. Apskaičiuotas tiriamųjų *n*-Si bangolaidžių plačiajuostiškumas. Nustatyta, kad tirtų bangolaidžių plačiajuostiškumas beveik toks pat. Atlikti realiosios ir menamosios dalių išilginės kompleksinės sklidimo konstantos ir skersinės sklidimo ore konstantos tyrimai, plačiame dažnių intervale nuo 15 iki 300 GHz. Nustatyta, kad dispersinės kreivės pabūdis priklauso nuo bangolaidžio spindulio. HE_{11} tipo bangos pobūdis, esant bangolaidžio spinduliui 0,25 mm ir bangos dažniui nuo 15 GHz iki 100 GHz, lieka nepakitęs. Parodyta, kad dažnių intervale, kai išilginės komleksinės sklidimo konstantos h' realioji dalis yra mažesnė už bangos skaičių *k*, nuostoliai bangolaidyje staigiai sumažėja. Il. 7, bibl. 8 (anglų kalba; santraukos anglų, rusų ir lietuvių k.).

DOI: 10.5755/j02.eie.10105